HHS Public Access

Author manuscript

Sci Transl Med. Author manuscript; available in PMC 2017 February 06.

Published in final edited form as:

Sci Transl Med. 2015 February 11; 7(274): 274ra18. doi:10.1126/scitranslmed.aaa0835.

Normalization of CD4+ T Cell Metabolism Reverses Lupus

Yiming Yin[1], **Seung-Chul Choi**[1], **Zhiwei Xu**[1], **Daniel J. Perry**[1], **Howard Seay**[1], **Byron P. Croker**[1], **Eric S. Sobel**[2], **Todd M. Brusko**[1], and **Laurence Morel**[1,*]

[1]Department of Pathology, Immunology, and Laboratory Medicine, Department of Medicine University of Florida, Gainesville, FL 32610, USA

[2]Division of Rheumatology and Clinical Immunology, Department of Medicine University of Florida, Gainesville, FL 32610, USA

Abstract

Systemic Lupus Erythematosus (SLE) is an autoimmune disease in which autoreactive $CD4^+$ T cells play an essential role. $CD4^+$ T cells rely on glycolysis for inflammatory effector functions, but recent studies have shown that mitochondrial metabolism supports their chronic activation. How these processes contribute to lupus is unclear. Here, we show that both glycolysis and mitochondrial oxidative metabolism are elevated in $CD4^+$ T cells from lupus-prone B6.*Sle1.Sle2.Sle3* (TC) mice as compared to non-autoimmune controls. *In vitro*, both the mitochondrial metabolism inhibitor metformin and the glucose metabolism inhibitor 2-Deoxy-D-glucose (2DG) reduced IFNγ production, although at different stages of activation. Metformin also restored the defective IL-2 production by TC $CD4^+$ T cells. *In vivo*, treatment of TC mice and other lupus models with a combination of metformin and 2DG normalized T cell metabolism and reversed disease biomarkers. Further, $CD4^+$ T cells from SLE patients also exhibited enhanced glycolysis and mitochondrial metabolism that correlated with their activation status, and their excessive IFNγ production was significantly reduced by metformin *in vitro*. These results suggest that normalization of T cell metabolism through the dual inhibition of glycolysis and mitochondrial metabolism is a promising therapeutic venue for SLE.

Introduction

$CD4^+$ T cells are active mediators of systemic lupus erythematosus (SLE) pathogenesis. Autoreactive nucleosome-specific T cells provide help to anti-DNA-specific B cells in mice *(1)* and SLE patients *(2)*. Lupus-prone mice carry large numbers of activated T cells *(3)* and signaling defects have been found in SLE $CD4^+$ T cells *(4)*. In addition, SLE patients and lupus-prone mice show an increase in Th1 and Th17 subsets (*5*), as well as a dysregulated expression of IFNγ and IL-2 *(6-8)*.

* Corresponding author: Laurence Morel, Department of Pathology, Univ. of Florida, 1395 Center Drive, Gainesville, FL 32610-0275. Tel: (352) 273-5638. Fax: (352) 392-3053. morel@ufl.edu.

Author contributions: YY, TB, and LM conceived and designed the experiments; YY; SCC; ZX; DJP; and HS performed the experiments; YY; SCC; DJP; BPC; TB; and LM analyzed data; ESS contributed materials/samples; YY LM wrote the paper.

Competing interests: YY and LM have filed a patent application entitled “Treatment of murine lupus with metabolic modulators” (UF#15055).

The activation, proliferation and differentiation of $CD4^+$ T cells are tightly regulated by cellular metabolism. Quiescent T cells have a low energy demand and can interchangeably use glucose, lipid and amino acids to fuel oxidative metabolism *(9, 10)*. Activation through the T cell receptor increases both glycolysis and mitochondrial metabolism (*11-14*) The upregulation of glycolysis results from a transcriptional reprogramming regulated by c-MYC, HIF1α and ERRα (*12, 15, 16*). The importance of glucose metabolism in autoimmunity was demonstrated by the overexpression of the glucose transporter *Glut1* in mice that led to $CD4^+$ T cell hyperactivation, hypergammaglobulinemia and immune complex mediated nephritis (*17*). Cellular metabolism also regulates effector T cell differentiation and memory cell formation. Th1, Th2, and Th17 cells express are highly glycolytic, whereas $Foxp3^+$ regulatory T cells (Tregs) and long-lived memory T cells have high lipid oxidation rates (*18, 19*).

Several studies have suggested that SLE $CD4^+$ T cells present defective mitochondrial functions. Splenocytes from (NZB X NZW)F1 (NZB/W) mice showed an enhanced pyruvate oxidation (*20*). Moreover, mitochondrial membrane hyperpolarization was associated with an elevated mTOR activity in $CD4^+$ T cells from SLE patients (*21*). Accordingly, SLE patients treated with rapamycin showed reduced disease manifestations (*22*). Furthermore, $CD4^+$ T cells employ oxidative metabolism for chronic activation in response to alloantigens (*23*), and ATP synthase inhibitors eliminated pathogenic T cells (*23, 24*). Given these conflicting results between the preponderance of either glycolysis or mitochondrial metabolism to support the function of activated effector T cells, the metabolism of SLE $CD4^+$ T cells remains poorly understood.

The B6.*Sle1.Sle2.Sle3* lupus-prone mouse model (a triple congenic strain hereafter called TC) contains three NZM2410-derived lupus susceptibility loci, *Sle1*, *Sle2* and *Sle3* on a non-autoimmune C57BL/6 (B6) background *(25).* TC mice spontaneously develop symptoms similar to SLE patients, including the production of anti-dsDNA IgG and a high penetrance of immune-complex mediated fatal glomerulonephritis (GN). The *Sle1c2* susceptibility locus corresponds to the reduced expression of the Estrogen Related Receptor Gamma (*Esrrg*) gene, which contributes to $CD4^+$ T cell activation and increased IFNγ secretion (*26*). *Esrrg* controls cellular metabolism by upregulating mitochondrial oxidative phosphorylation (OXPHOS) *(27, 28)*. This finding led us to hypothesize that cellular metabolism contributes to lupus pathogenesis through T cell activation, and that metabolism modulators could be used to reduce or revert disease. We tested this hypothesis in TC mice, which express *Sle1c2*, as well as with $CD4^+$ T cells from SLE patients. Here, we show that both glycolysis and mitochondrial oxygen consumption are elevated in $CD4^+$ T cells from TC mice. This enhanced metabolism was observed in naïve T cells, and was amplified with age and activation. *In vitro*, treatment with mitochondrial electron transport chain complex I inhibitor metformin (Met) or glucose metabolism inhibitor 2DG normalized IFNγ production by TC $CD4^+$ T cells. *In vivo*, treatment of TC mice and other lupus models with the combination of Met and 2DG normalized T cell metabolism and reversed disease phenotypes. We also demonstrated that $CD4^+$ T cells from SLE patients exhibited both a higher glycolysis and mitochondrial metabolism as compared to healthy controls, which correlated with T cell activation and subset distribution. Moreover, their excessive IFNγ

production was significantly reduced by Met *in vitro*. These results suggest that targeting T cell metabolism represents a promising therapeutic strategy for SLE.

Results

CD4+ T cells from TC mice exhibited elevated T cell metabolism

TC $CD4^+$ T cells present with several immune abnormalities that are typical of lupus pathogenesis *(25, 29),* including T cell hyperactivation (Fig. S1A and Fig. 5B), accumulation of $CD44^+CD62L^-$ effector memory (Tem) and $CD44^+CD62L^+$ central memory T (Tcm) cells (Fig. S1B and Fig. 5C), as well as increased IFNγ production (Fig. S1C and Fig. 3H). To test whether these $CD4^+$ T cell phenotypes were associated with alterations in cellular metabolism, we measured their extracellular acidification rate (ECAR), which is primarily attributed to glycolysis, and the oxygen consumption rate (OCR), which corresponds to OXPHOS. $CD4^+$ T cells from 2 month old pre-disease TC mice showed enhanced ECAR and OCR compared to age-matched B6 counterparts. This difference in $CD4^+$ T cell metabolism became more pronounced in 9 month old TC mice, which have developed clinical disease (Fig. 1A-C). $CD4^+$ T cells from 9 month old TC mice also showed a higher spare respiratory capacity (SRC) (Fig. 1D), an indication of cellular energy reserve that is essential for memory T cell formation and function *(30)*. The enhanced glycolysis of TC $CD4^+$ T cells was confirmed by increased extracellular lactate production (Fig. 1E). In spite of increased glycolysis and OXPHOS, TC $CD4^+$ T cells presented intracellular ATP levels comparable to B6, both *ex vivo* and after activation (Fig. 1F). This result suggests that the increased metabolism leads to ATP consumption by TC $CD4^+$ T cells to support elevated effector functions. Overall, $CD4^+$ T cells from TC mice present with an enhanced cellular metabolism that precedes disease manifestation and increases as T cells become more activated and disease progresses.

Naïve and activated $CD4^+$ T cell subsets have different metabolic profiles *(31)*. The expansion of Tem cells in TC mice (Fig. S1B) could be the source of the elevated metabolism observed in total $CD4^+$ T cells. Tem cells showed a significantly higher ECAR and, to a lesser extent, OCR, than Tn cells in both B6 and TC mice (Fig. 1G and H). This result implies that the higher percentage of Tem cells in TC mice contributes to the higher metabolism of total $CD4^+$ T cells. In addition, TC Tn cells also showed a higher ECAR and OCR than B6 Tn cells. To directly characterize the metabolism of TC $CD4^+$ T cells after activation, we compared the metabolic profiles of B6 and TC sorted Tn cells following stimulation with anti-CD3 and anti-CD28 for 24 h. *In vitro* stimulated TC Tn cells exhibited significantly higher ECAR and OCR as compared to B6 (Fig. 1I and J). The activity of mTORC1, a sensor for cellular energy (*32*), was elevated in TC $CD4^+$ T cells, as shown by an increased phosphorylation of S6 and 4E-BP1, and the increased expression of CD98 and CD71 (Fig. 2A and Fig. S2). The mTORC1 inhibitor rapamycin reduced glycolysis and mitochondrial oxygen consumption in anti-CD3/CD28 activated B6 $CD4^+$ T cells (Fig. 2B), linking mTORC1 activity to both glycolysis and mitochondrial metabolism. These results indicate that naïve TC $CD4^+$ T cells exhibit both an increased glycolysis and mitochondrial oxygen consumption *ex vivo* and in response to *in vitro* activation.

TC CD4$^+$ T cells showed an elevated expression of glycolytic genes *Hif1a*, *Hk2*, and *Slc16a3*, (Fig. S2A). On the other hand, the level of *Pdk1,* which inhibits pyruvate oxidation, was significantly lower in TC than B6 CD4$^+$ T cells (Fig. S2B). The expression of *Cpt1a*, a key FAO regulator *(30),* was higher in TC CD4$^+$ T cells than in B6 (Fig. S2C). Consistently, TC CD4$^+$ T cells showed an enhanced uptake of fatty acids (Fig. S2D). Finally, TC CD4$^+$ T cells showed a higher expression of *Gls2* and *Odc* (Fig. S2E), two genes involved in amino acid metabolism *(12)*. In summary, CD4$^+$ T cells from lupus-prone TC mice present an enhanced metabolism fueled through both glycolysis and mitochondrial metabolism, with evidence that glucose, fatty acids and glutamine may all contribute to the latter.

TC CD4$^+$ T cell dysfunction was normalized by metabolic modulators *in vitro*.

We tested whether targeting glycolysis and mitochondrial metabolism could normalize TC CD4$^+$ T cell functions *in vitro*. As expected, 2DG dose-dependently inhibited CD4$^+$ T cell ECAR (Fig. 3A), but also decreased OCR (Fig. 3B), presumably by decreasing glucose oxidation. Consistent with its inhibition of mitochondrial complex I (*33*), Met dose-dependently decreased OCR (Fig. 3C) and increased ECAR at a high concentration (Fig. 3D), likely as an alternative pathway to generate ATP. We examined whether IFNγ production could be modulated by Met or 2DG *in vitro*. TC CD4$^+$ T cells produced more IFNγ than B6 T cells after a short stimulation with PMA/Ionomycin, which was decreased by treatment with Met (Fig. 3E). The ATPase inhibitor oligomycin and the combination of Complex I/III inhibitors Retonone/Antimycin A also inhibited IFNγ production, indicating that mitochondrial metabolism is required for IFNγ production during early CD4$^+$ T cell activation. 2DG, however, had no effect, indicating that IFNγ production does not rely on glycolysis at that stage. Under Th1 polarizing condition, TC CD4$^+$ T cells also generated more IFNγ than B6 T cells (Fig. 3F). Met added at the beginning of the culture dose-dependently decreased IFNγ production (Fig. 3F), which could be observed as early as day 1 and throughout the 3 day culture (Fig. 3G). When added at day 2 of polarization, Met had no effect, whereas 2DG dramatically reduced IFNγ production in both strains (Fig. 3H). These results show that, in both normal and lupus mice, IFNγ production by CD4$^+$ T cells depends on mitochondrial metabolism in the activation phase when it can be reduced by Met, whereas its production during the proliferation phase depends on glycolysis and can be reduced by 2DG.

IL-2 production is defective in lupus T cells (*7*). Anti-CD3/CD28 stimulated TC CD4$^+$ T cells produced less IL-2 than B6 T cells and Met treatment increased IL-2 production in both strains in a dose-dependent manner (Fig. 3I-J and Fig. S4). In summary, TC CD4$^+$ T cells display excessive IFNγ as well as a defective IL-2 secretion. Both Met and 2DG inhibited their capacity to produce IFNγ, but at different stages of activation and Met promoted IL-2 production. This resulted in an overall normalization of TC CD4$^+$ T cell functions *in vitro*.

A treatment combining Met and 2DG reversed disease in TC mice

To target glucose metabolism and mitochondrial metabolism simultaneously, we treated 7 month old TC mice with a combination of 2DG and Met (Met+2DG) in drinking water for 3 months. At that age, TC mice are at the early stage of clinical disease that includes splenomegaly, anti-dsDNA IgG production, accumulation of activated T (Fig. S1) and B

cells, as well as splenic plasma cells (*25*). The Met+2DG treatment significantly decreased ECAR (Fig. 4A) and OCR (Fig. 4B) in TC $CD4^+$ T cells to levels similar to that of B6 T cells, indicating that the treatment effectively targeted $CD4^+$ T cell metabolism *in vivo*. B6 $CD4^+$ T cells were however not affected, suggesting that the treatment is selective to the more metabolically-active TC cells. A further characterization showed that the *in vivo* treatment selectively downregulated metabolism in TC effector T cells (Fig. S5). The Met +2DG treatment significantly reduced splenomegaly in TC mice, but had little effect in B6 mice (Fig. 4C). Importantly, the treatment significantly decreased the production of anti-dsDNA IgG and anti-nuclear autoantibodies (ANA), while it increased in untreated TC mice (Fig. 4D-E). The inhibitory effect of the treatment on autoantibody production was confirmed with antigens arrays, in which 4 out of 5 treated TC mice showed a profile similar to B6 mice (Fig. 4F). The Met+2DG treatment also reduced the level of C3 and IgG2a immune complex deposition in TC kidneys (Fig. 4G). Furthermore, GN was less severe in treated TC mice, either assessed by severity rank or by score distribution (Fig. 4H and I).

Met+2DG decreased the percentage of total splenic $CD4^+$ T cells in TC mice (Fig. 5A), as well as activation measured as the percentages of $CD69^+$ expression (Fig. 5B) and Tem (Fig. 5C-D). Globally, Met+2DG decreased the expression of markers associated with activation and effector functions in TC $CD4^+$ T cells, and increased their expression of the inhibitory molecule CTLA-4 (Fig. S6). For most markers, the expression level on $CD4^+$ T cells from treated TC mice was similar to that of age-matched B6 mice. Both follicular helper (Tfh) and follicular regulatory (Tfr) T cell subsets were reduced in TC spleens after Met+2DG treatment (Fig. 5E-G), which reflects the overall decrease in FO T cells. The expression levels of PD1, CXCR5, and BCL6 were drastically reduced by the treatment (Fig. S6).Within the FO T cells, the treatment expanded Tfr at the expense of Tfh population ($P = 0.04$). The high frequency of GC B cells in TC mice (*35*) was also reduced after treatment (Fig. 5H). Finally, Met+2DG restored the impaired production of IL-2 by TC $CD4^+$ T cells (Fig. 5I), and reduced mTORC1 activity (Fig. 5J-M). In conclusion, Met+2DG treatment resulted in a profound and global reversal of T cell activation in TC mice, while it had minimal effects on B6 T cells.

Met+2DG-treated TC and B6 mice maintained their body weight and blood glucose (Fig.S7). The treatment did not result in a general humoral suppression since total serum IgM and IgG were unchanged in TC mice (Fig. S8A). The reason for the increased total IgG in treated B6 mice is not clear at this point. Furthermore, Met+2DG treatment did not impair the humoral response in response to a foreign antigen (Fig. S8B). Met+2DG-treated B6 mice immunized with NP-KLH produced the same amount of anti-NP IgM and IgG1 with no difference in affinity or kinetics. The number of B cells, GC B cells and plasma cells (Fig. S8C), Tem $CD4^+$ T cells, Tfh cells and Tfr cells, as well as their expression of effector surface markers were similar between treated and untreated mice (Fig. S8D-E). A one-month treatment also decreased the metabolism of TC $CD4^+$ T cells (Fig. S9A and B) and there was a trend for the reduction of spleen size (Fig. S9C). The treatment reduced the production of anti-dsDNA IgG (Fig. S9D) and ANA (Fig. S9E-F), the percentage of $CD4^+$ T cells (Fig. S9G), $CD4^+$ T cell activation (Fig. S9H-I) as well as the percentage of GC B cells (Fig. S9J). The short-term treatment also decreased glomerular IgG2a immune complexes

(Fig. S7K-L), and improved renal pathology (Fig. S9M-N). Thus, one month of Met+2DG treatment reversed disease biomarkers in TC mice.

Met +2DG treatment reversed disease phenotypes in other mouse models of SLE

We tested how Met+2DG treatment impact disease phenotypes in two additional models of SLE. A 1-month Met+2DG treatment of 7-month old NZB/W mice reduced their $CD4^+$ T cell metabolism, although the difference was significant only for OCR (Fig. 6A-B). It also decreased the production of anti-dsDNA IgG (Fig. 6C) and tended to reduce serum ANA levels, despite an increase in control mice (Fig. 6D). Contrary to TC mice, Met+2DG significantly decreased total IgG (Fig. 6F) and there was a trend in the same direction for IgM (Fig. 6E). The total $CD4^+$ T cell percentage was unaffected by treatment (Fig. 6G), but $CD4^+$ T cell activation (Fig. 6H), the percentage of Tem (Fig. 6 I), Tfh and Tfr $CD4^+$ T cells (Fig. 6J-K), as well as GC B cells (Fig. 6L) and mTROC1 activity (Fig. 6M-P) were all decreased in treated NZB/W mice. Renal pathology was however unchanged (Fig. 6 Q-R). Thus, a 1-month Met+2DG treatment reversed the immunophenotypes of NZB/W mice.

The impact of Met+2DG treatment was also assessed in the cGVHD induced model of lupus (*36*). Treatment did not affect the induced splenomegaly (Fig. S10A), but it reduced the production of anti-dsDNA IgG (Fig. S10B), as well as the percentage of Tcm, but not Tem $CD4^+$ T cells (Fig. S10C-D). Therefore, Met+2DG prevented the induction of T-cell dependent production of autoantibodies. Met monotherapy reduced splenomegaly (Fig. S10A) and the size of the memory T cell subset (Fig. S10C-D) in this model, it had no effect on the induction of anti-dsDNA IgG (Fig. S10B). This suggested that the combination of the two metabolic inhibitors is required for the effective suppression of autoimmunity.

Metformin and 2DG showed a synergic effect *in vivo*

We evaluated the relative contributions of 2DG and Met to disease reversal in 7-month old TC mice treated for one month at the same dose used for the combination treatment. 2DG decreased ECAR but had no effect on OCR in TC $CD4^+$ T cells (Fig. S11A-B). We did not observe any effect on spleen weight (Fig. S11C), autoantibodies production (Fig. S11D-F), $CD4^+$ T frequency (Fig. S11G), $CD4^+$ T and B cell activation, or effector subset distribution in these treated mice (Fig. S11H-L). Although 2DG lowered immune complex deposition in the kidneys (Fig. S11M-N), renal pathology was not ameliorated (Fig. S11O-P). Met monotherapy did not alter either ECAR or OCR in TC $CD4^+$ T cells (Fig. S12A-B), or any of the biomarkers that were affected by the combination treatment (Fig. S12C-N). Therefore, one month treatment of neither 2DG or Met alone had an effect on the established autoimmune pathology of TC mice. Although it is possible that monotherapy for a longer time could have stronger effect on the disease, it is clear that Met+2DG treatment is superior than Met or 2DG alone, which strongly suggests a synergistic effect between 2DG and Met in reversing lupus phenotypes.

$CD4^+$ T cells from SLE patients exhibited elevated cellular metabolism

SLE patients present with a reduced percentage of naïve $CD4^+CD45RA^+CCR7^+$ T cells and a corresponding increase in $CD4^+CD45RA^-CCR7^+$ central memory T cells, leading to an altered ratio of Tn/Tcm subsets as compared to healthy controls (HCs) (Fig. S13A-D, F). No

significant difference was found in the percentage of circulating $CD4^+CD127^{-/lo}CD25^+$ Tregs (Fig. S11E, G). We compared ECAR, OCR and SRC in $CD4^+$ T cells purified from peripheral blood of SLE patients and HCs, with and without anti-CD3 and anti-CD28 activation (Fig. 7A-B). Given that the SLE patients were treated with at least one immunosuppressive drug (Table S1), we tested whether three of the most commonly used drugs could affect $CD4^+$ T cell metabolism. HC $CD4^+$ T cells were treated for 24 h with either dexamethasone (Dex), hydroxychloroquine (HCQ) or mycophenolate mofetil (MMF) at a concentration that did not affect cell viability. Dex inhibited ECAR but not OCR, whereas HCQ and especially MMF reduced both ECAR and OCR (Fig. S13H-I). Despite the decreased metabolism induced by these treatments, activated $CD4^+$ T cells showed a higher ECAR in SLE than HC samples (Fig. 7C), and both resting and activated SLE $CD4^+$ T cells showed a OCR than HC T cells (Fig. 7D). Notably, anti-CD3/CD28 activation induced a rapid increase in both ECAR and OCR (Figure 7A and B), suggesting that both pathways are important for the early activation of human $CD4^+$ T cells. Moreover, both resting and activated SLE $CD4^+$ T cells have a significantly higher SRC (Fig. 7B and E). These metabolic parameters were correlated with the distribution of circulating $CD4^+$ T cell subsets. The percentage of Tn was inversely correlated with both activated ECAR (Fig. 7F) and basal OCR (Fig. 7G) levels, while the percentage of Treg was positively correlated with activated ECAR (Fig. 7H). These results strongly suggest that, as shown in the mouse, cellular metabolism regulates human $CD4^+$ T cell activation and effector functions. Further, our results show a strong association between a dysregulated homeostasis in SLE $CD4^+$ T cells and an elevated cellular metabolism. Consistently with our findings in mice (Fig. 3), SLE $CD4^+$ T cells produced more IFNγ than HCs after Th1 induction (Fig. 7I). Met decreased IFNγ production from SLE and HC $CD4^+$ T cells to comparable levels between the two cohorts (Fig. 7I). Overall, these results showed that Met treatment normalized the *in vitro* IFNγ production by SLE $CD4^+$ T cells.

Discussion

$CD4^+$ T cells upregulate glycolysis following activation, a phenomena very similar to the Warburg effect described in cancer cells *(37)*. Glycolysis is critical for T cell effector functions, and increased glycolysis leads to autoimmunity (*13, 17*). More recently, the field has gained a better appreciation for mitochondrial oxidative metabolism in mediating T cell activation and proliferation *(12, 14, 23)*. Here, we showed that $CD4^+$ T cells from the TC lupus model as well as from SLE patients exhibit elevated glycolysis and mitochondrial oxidative metabolism as compared to non-autoimmune controls, both *ex vivo* and after *in vitro* activation. We also showed that the enhanced oxidative metabolism is attributed to a combination of higher glucose, fatty acids and glutamine oxidation. Moreover, the enhanced metabolism in $CD4^+$ T cells is associated with an increased mTORC1 activity. These findings led us to hypothesize that lupus could be treated with metabolic modulators that target both glycolysis and mitochondrial metabolism. We found that treating TC mice with a combination of Met and 2DG normalized T cell metabolism and reversed disease phenotypes, including T cell activation, autoantibody production, and renal disease. The combination treatment was also effective on the NZB/W spontaneous lupus model and the

cGVHD induced model. This result suggests that dysregulated T cell metabolism may be underlying SLE pathogenesis and T cell metabolism can be a therapeutic target.

Metabolic modulators have been evaluated for a number of diseases. Rapamycin reduced disease activity in MRL/lpr mice *(38)* and in SLE patients *(22)*. Treatment with N-acetylcysteine, a precursor of gluthatione that blocks mTOR, improved disease outcomes in NZB/W mice *(39)* and SLE patients *(40)*. A clinically approved inhibitor of glycosphingolipids biosynthesis, N-butyldeoxynojirimycin, normalized the functions of $CD4^+$ T cells from SLE patients *(41)*. Met is commonly used to treat type 2 diabetes, and 2DG has been tested to treat cancer *(42)* and Alzheimer's disease *(43)*. Interestingly, either 2DG or Met alone inhibited the development of experimental autoimmune encephalomyelitis, a mouse model of multiple sclerosis (*13, 44*). 3PO, a small molecule inhibitor of PFKFB3, an enzyme that controls a rate limiting step of glycolysis, prevented the development of T cell-mediated delayed-hypersensitivity and imiquimod-induced psoriasis in the mouse (*45*). To the contrary, we showed in this study that a dual inhibition of glycolysis and mitochondrial metabolism synergizes for the reversal of lupus in the TC model, which highlighted the complexity of this disease. A synergistic effect of Met and 2DG has been shown in cancer models *(46)*. As recent studies have revealed the importance of glycolysis and mitochondrial metabolism in controlling T cell effector functions, dual inhibition of glycolysis and mitochondrial metabolism may have broader applications to other immune mediated diseases besides lupus.

Our study provides possible mechanisms by which Met and 2DG reversed immunophenotypes *in vivo*. Met regulates cellular metabolism through complex mechanisms (*47*), including the inhibition of the mitochondrial respiratory chain complex I (*33*). In this study, the Met+2DG treatment decreased T cell mitochondrial oxygen consumption as well as mTORC1 signaling in both the TC and NZB/W models. Therefore, inhibiting mitochondrial metabolism and antagonizing mTOR signaling are the likely mechanisms by which Met normalized TC $CD4^+$ T cell metabolism *in vivo*. We also observed a decrease in glycolysis after the Met+2DG treatment, which is likely the mechanism by which 2DG normalized TC $CD4^+$ T cell metabolism *in vivo*.

In summary, we have identified defective $CD4^+$ T cell metabolism as a therapeutic target in both murine and human SLE. Besides $CD4^+$ T cells, Met+2DG may also target directly other immune cell types *in vivo*. Glucose metabolism is essential for B cell functions *(48)*. Both glycolysis and mitochondrial metabolism are important for the activation and maturation of dendritic cells (*49, 50*), which can indirectly affect T cells. It will be important to find out whether lupus mice have abnormal metabolism in other immune cell compartments, and whether the metabolism of those cells is altered after Met+2DG treatment *in vivo*. Although Met+DG was effective at reversing disease phenotypes while the monotheraphies at the same doses were not, it is possible that different doses or a longer duration would be effective for either Met or 2DG alone. We have also not yet investigated whether the treatment needs to be maintained to prevent flares, or whether it resets the immune system for an extended period of time. Another limitation of the present study is that 2DG blocks the entire glucose metabolic pathway and does not discriminate between the contribution of glycolysis and glucose oxidation. Finally, a comprehensive evaluation of

the effect of Met, with and without glucose inhibitors, on the functions of human $CD4^+$ T cells should be performed.

Methods

Study design

The objective of the study was to define the metabolism of mouse and human SLE $CD4^+$ T cells and to explore potential metabolism-based therapeutic strategies. The metabolism of mouse $CD4^+$ T cells was first evaluated ex vivo and after *in vitro* stimulation in presence of metabolic inhibitors. Six to seven-month old anti-dsDNA IgG positive lupus mice and age-matched B6 controls were randomized to treatment and control groups. Treatment was performed for 1 or 3 months with Met (3 mg/mL) or 2DG (5 mg/mL), or a combination of the two, dissolved in drinking water. Age-matched control mice received plain drinking water. Peripheral blood was collected biweekly to analyze autoantibody production; body weight and blood sugar levels were monitored weekly and biweekly respectively. At the end of the treatment, spleens were collected for flow cytometry and metabolic analysis of $CD4^+$ T cells, and kidneys were evaluated for renal pathology in a blinded fashion. All experiments were conducted according to protocols approved by the University of Florida IACUC. For human subjects, at least 20ml of peripheral blood was obtained after signed informed consent in accordance with UF IRB. Female SLE patients fulfilled at least four of the revised SLE criteria of the American College of Rheumatology. Healthy female volunteers with no family history of autoimmune disease served as age and ethnicity-matched controls (HC). All patients were treated with at least one medication, none of them with a biologic treatment. The demographics and treatment regimens of the patients and HCs are summarized in Table S1.

Mice

TC mice have been described previously (18). C57BL/6J (B6), B6(C)-H2-Ab1bm12/KhEgJ mice and (NZB x NZW)F1 mice were purchased from the Jackson Laboratory. Only female mice were used in this study. Chronic graft-versus-host disease (cGVHD) was induced as previously described *(29).*

Metabolic measurements

Splenocyte suspensions were enriched for $CD4^+$ T cells by negative selection with magnetic beads (Miltenyi). Naïve (Tn: $CD4^+CD44^-CD62L^+$) and effector memory (Tem: $CD4^+CD44^+CD62L^-$) subsets were sorted with a FACSAria cell sorter (BD Biosciences). Sorted mouse Tn were activated with plate-bound anti-CD3e (145-2C11, 2 ug/mL) and soluble anti-CD28 (37.51, 1 ug/mL) for 24 h. ECAR and OCR were measured using either a XF24 or a XF96 Extracellular Flux Analyzers under mitochondrial stress test conditions (Seahorse). Assay buffer was made of non-buffered RPMI medium (Sigma) supplemented with 2.5 uM dextrose, 2 mM glutamine and 1 uM Sodium Pyruvate. Baseline ECAR and OCR values were averaged between technical replicates for these first 3 successive time intervals. Extracellular lactate production was measured using L-Lactate Assay Kit (Abcam). Intracellular ATP was measured using the ATP Determination Kit (Life

Technologies). Fatty acid uptake by $CD4^+$ T cells was measured by flow cytometry with the Bodipy dye (Life Technology).

Gene Expression Analysis

SybrGreen (Applied Biosystems)-based quantitative PCR was performed on cDNA from bead-enriched $CD4^+$ T cells with primer sequences shown in Table S2. mRNA levels were expressed as Relative Quantities (RQ) to *Ppia* (cyclophylin A).

Flow Cytometry

The immunophenotypes of human $CD4^+$ T cells were determined with antibody panels emulated by the Human Immunophenotyping consortium (57). The other antibodies used in this study are listed in Table S3. Cytokine production was analyzed in cells treated with the leukocyte activation cocktail (BD Biosciences) and the Fixation/Permeabilization kit (eBiosciences).

Cell Culture

Mouse splenic $CD4^+$ T cells were stimulated by anti-CD3e and anti-CD28 for 3 d and IL-12 (10 ng/ml) for Th1 differentiation. IL-2 was measured in $CD4^+$ T cells stimulated by anti-CD3e and anti-CD28. Human $CD4^+$ T cells were enriched from peripheral blood using the RosetteSep® Enrichment Cocktail (StemCell Technologies). For Th1 polarization, cells were stimulated in cRPMI with beads coated with anti-CD3 and anti-CD28 (Dynabeads Human T-Activator, Life Technologies) for 6 d with IL-12 (10 ng/ml), IL-2 (20 U) and anti-IL-4 (1 ug/ml).. In some assays, dexamethasone, hydroxychloroquine or mycophenolate mofetil (1 uM, Sigma) was added and ECAR and OCR were measured 24 h later.

Antibody measurement

Serum anti-dsDNA, anti-chromatin IgG and ANA were measured as previously described *(25).* Autoantibody microarray analysis was performed at the Microarray Core Facility in University of Texas Southwestern Medical Center.

Renal pathology

Glomerulonephritis was scored and the glomerular deposition of C3 and IgG2a immune complexes was evaluated on frozen kidney sections as previously described (*51*).

Statistical Analysis

Statistical analyses were performed using the GraphPad Prism 6.0 software. Unless indicated, data was normally distributed, and graphs show means and standard deviations of the mean (SEM) for each group and results were compared with 2-tailed *t* tests with a level of significant of $P < 0.05$. Bonferroni corrections were applied for multiple comparisons. Each *in vitro* experiment was performed at least twice with reproducible results.

Supplementary Material

Refer to Web version on PubMed Central for supplementary material.

Acknowledgements

We thank Dr. Clayton Mathews for helpful suggestions, Nathalie Kanda and Leilani Zeumer for expert technical help.

Funding: Supported by NIH grants R01 AI045050 and ALR-TIL 0000075018 (to L. Morel).

References

1. Mohan C, Adams S, Stanik V, Datta SK. Nucleosome: a major immunogen for pathogenic autoantibody-inducing T cells of lupus. J. Exp. Med. 1993; 177:1367–1381. [PubMed: 8478612]
2. Kang HK, Chiang MY, Liu M, Ecklund D, Datta SK. The histone peptide H4 71-94 alone is more effective than a cocktail of peptide epitopes in controlling lupus: immunoregulatory mechanisms. J. Clin. Immunol. 2011; 31:379–394. [PubMed: 21287397]
3. Kong PL, Odegard JM, Bouzahzah F, Choi JY, Eardley LD, Zielinski CE, Craft JE. Intrinsic T cell defects in systemic autoimmunity. Ann. N.Y. Acad. Sci. 2003; 987:60–67. [PubMed: 12727624]
4. Crispín JC, Kyttaris VC, Juang YT, Tsokos GC. How signaling and gene transcription aberrations dictate the systemic lupus erythematosus T cell phenotype. Trends Immunol. 2008; 29:110–115. [PubMed: 18249583]
5. Apostolidis SA, Lieberman LA, Kis-Toth K, Crispín JC, Tsokos GC. The dysregulation of cytokine networks in systemic lupus erythematosus. J. Interferon Cytokine Res. 2011; 31:769–779. [PubMed: 21877904]
6. Theofilopoulos AN, Koundouris S, Kono DH, Lawson BR. The role of IFN-gamma in systemic lupus erythematosus: a challenge to the Th1/Th2 paradigm in autoimmunity. Arthritis Res. 2001; 3:136–141. [PubMed: 11299053]
7. Ohl K, Tenbrock K. Inflammatory cytokines in systemic lupus erythematosus. J. Biomed. Biotechnol. 2011; 2011:432595. [PubMed: 22028588]
8. Pollard KM, Cauvi DM, Toomey CB, Morris KV, Kono DH. Interferon-gamma and systemic autoimmunity. Discov. Med. 2013; 16:123–131. [PubMed: 23998448]
9. Fox CJ, Hammerman PS, Thompson CB. Fuel feeds function: energy metabolism and the T-cell response. Nat. Rev. Immunol. 2005; 5:844–852. [PubMed: 16239903]
10. Pearce EL, Poffenberger MC, Chang CH, Jones RG. Fueling immunity: insights into metabolism and lymphocyte function. Science. 2013; 342:1242454. [PubMed: 24115444]
11. Frauwirth KA, Riley JL, Harris MH, Parry RV, Rathmell JC, Plas DR, Elstrom RL, June CH, Thompson CB. The CD28 signaling pathway regulates glucose metabolism. Immunity. 2002; 16:769–777. [PubMed: 12121659]
12. Wang R, Dillon C-P, Shi L-Z, Milasta S, Carter R, Finkelstein D, McCormick L-L, Fitzgerald P, Chi H, Munger J, Green D-R. The transcription factor Myc controls metabolic reprogramming upon T lymphocyte activation. Immunity. 2011; 35:871–882. [PubMed: 22195744]
13. Shi LZ, Wang R, Huang G, Vogel P, Neale G, Green DR, Chi H. HIF1alpha-dependent glycolytic pathway orchestrates a metabolic checkpoint for the differentiation of TH17 and Treg cells. J. Exp. Med. 2011; 208:1367–1376. [PubMed: 21708926]
14. Sena LA, Li S, Jairaman A, Prakriya M, Ezponda T, Hildeman DA, Wang CR, Schumacker PT, Licht JD, Perlman H, Bryce PJ, Chandel NS. Mitochondria are required for antigen-specific T cell activation through reactive oxygen species signaling. Immunity. 2013; 38:225–236. [PubMed: 23415911]
15. Dang E-V, Barbi J, Yang HY, Jinasena D, Yu H, Zheng Y, Bordman Z, Fu J, Kim Y, Yen HR, Luo W, Zeller K, Shimoda L, Topalian S-L, Semenza G-L, Dang C-V, Pardoll D-M, Pan F. Control of TH17/Treg balance by hypoxia-inducible factor 1. Cell. 2011; 146:772–784. [PubMed: 21871655]
16. Michalek RD, Gerriets VA, Nichols AG, Inoue M, Kazmin D, Chang CY, Dwyer MA, Nelson ER, Pollizzi KN, Ilkayeva O, Giguere V, Zuercher WJ, Powell JD, Shinohara ML, McDonnell DP, Rathmell JC. Estrogen-related receptor-à is a metabolic regulator of effector T-cell activation and differentiation. Proc.Natl. Acad. Sci. U.S.A. 2011; 108:18348–18353. [PubMed: 22042850]

17. Jacobs SR, Herman CE, MacIver NJ, Wofford JA, Wieman HL, Hammen JJ, Rathmell JC. Glucose uptake is limiting in T cell activation and requires CD28-mediated Akt-dependent and independent pathways. J. Immunol. 2008; 180:4476–4486. [PubMed: 18354169]
18. Michalek RD, Gerriets VA, Jacobs SR, Macintyre AN, MacIver NJ, Mason EF, Sullivan SA, Nichols AG, Rathmell JC. Cutting edge: distinct glycolytic and lipid oxidative metabolic programs are essential for effector and regulatory CD4+ T cell subsets. J. Immunol. 2011; 186:3299–3303. [PubMed: 21317389]
19. Pearce EL, Walsh MC, Cejas PJ, Harms GM, Shen H, Wang LS, Jones RG, Choi Y. Enhancing CD8 T-cell memory by modulating fatty acid metabolism. Nature. 2009; 460:103–107. [PubMed: 19494812]
20. Wahl DR, Petersen B, Warner R, Richardson BC, Glick GD, Opipari AW. Characterization of the metabolic phenotype of chronically activated lymphocytes. Lupus. 2010; 19:1492–1501. [PubMed: 20647250]
21. Fernandez DR, Telarico T, Bonilla E, Li Q, Banerjee S, Middleton FA, Phillips PE, Crow MK, Oess S, Muller-Esterl W, Perl A. Activation of mammalian target of rapamycin controls the loss of TCRzeta in lupus T cells through HRES-1/Rab4-regulated lysosomal degradation. J. Immunol. 2009; 182:2063–2073. [PubMed: 19201859]
22. Fernandez D, Bonilla E, Mirza N, Niland B, Perl A. Rapamycin reduces disease activity and normalizes T cell activation-induced calcium fluxing in patients with systemic lupus erythematosus. Arthritis Rheum. 2006; 54:2983–2988. [PubMed: 16947529]
23. Byersdorfer CA, Tkachev V, Opipari AW, Goodell S, Swanson J, Sandquist S, Glick GD, Ferrara JL. Effector T cells require fatty acid metabolism during murine graft-versus-host disease. Blood. 2013; 122:3230–3237. [PubMed: 24046012]
24. Gatza E, Wahl DR, Opipari AW, Sundberg TB, Reddy P, Liu C, Glick GD, Ferrara JLM. Manipulating the bioenergetics of alloreactive T cells causes their selective apoptosis and arrests graft-versus-host disease. Science Translational Medicine. 2011; 3:67ra68–67ra68.
25. Morel L, Croker BP, Blenman KR, Mohan C, Huang G, Gilkeson G, Wakeland EK. Genetic reconstitution of systemic lupus erythematosus immunopathology with polycongenic murine strains. Proc. Natl. Acad. Sci. U.S.A. 2000; 97:6670–6675. [PubMed: 10841565]
26. Perry DJ, Yin Y, Telarico T, Baker HV, Dozmorov I, Perl A, Morel L. Murine lupus susceptibility locus Sle1c2 mediates CD4+ T cell activation and maps to estrogen-related receptor γ. J. Immunol. 2012; 189:793–803. [PubMed: 22711888]
27. A. Alaynick W, P. Kondo R, He W. Xie, W. Dufour CR, Downes M, Jonker JW, Giles W, Naviaux RK, Giguére V, Evans RM. ERRgamma directs and maintains the transition to oxidative metabolism in the postnatal heart. Cell Metab. 2007; 6:13–24. [PubMed: 17618853]
28. Rangwala SM, Wang X, Calvo JA, Lindsley L, Zhang Y, Deyneko G, Beaulieu V, Gao J, Turner G, Markovits J. Estrogen-related receptor gamma is a key regulator of muscle mitochondrial activity and oxidative capacity. J. Biol. Chem. 2010; 285:22619–22629. [PubMed: 20418374]
29. Xu Z, Duan B, Croker BP, Morel L. STAT4 deficiency reduces autoantibody production and glomerulonephritis in a mouse model of lupus. Clin. Immunol. 2006; 120:189–198. [PubMed: 16713741]
30. van der Windt GJ, Everts B, Chang CH, Curtis JD, Freitas TC, Amiel E, Pearce EJ, Pearce EL. Mitochondrial respiratory capacity is a critical regulator of CD8+ T cell memory development. Immunity. 2012; 36:68–78. [PubMed: 22206904]
31. MacIver NJ, Michalek RD, Rathmell JC. Metabolic regulation of T lymphocytes. Annu. Rev. Immunol. 2013; 31:259–283. [PubMed: 23298210]
32. Yang K, Chi H. mTOR and metabolic pathways in T cell quiescence and functional activation. Sem. Immunol. 2012; 24:421–428.
33. Wheaton WW, Weinberg SE, Hamanaka RB, Soberanes S, Sullivan LB, Anso E, Glasauer A, Dufour E, Mutlu GM, Budigner GS, Chandel NS. Metformin inhibits mitochondrial complex I of cancer cells to reduce tumorigenesis. Elife. 2014; 3:e02242. [PubMed: 24843020]
34. Kaminski MM, Sauer SW, Klemke CD, Süss D, Okun JG, Krammer PH, Gülow K. Mitochondrial reactive oxygen species control T cell activation by regulating IL-2 and IL-4 expression:

mechanism of ciprofloxacin-mediated immunosuppression. J. Immunol. 2010; 184:4827–4841. [PubMed: 20335530]

35. Sang A, Niu H, Cullen J, Choi SC, Zheng YY, Wang H, Shlomchik MJ, Morel L. Activation of rheumatoid factor–specific B cells is antigen dependent and occurs preferentially outside of germinal centers in the lupus-prone NZM2410 mouse model. J. Immunol. 2014; 109:1609–1621.
36. Xu, Y., Zeumer, L., Reeves, W., Morel, L. Systemic Lupus Erythematosus. Eggleton, P., Ward, FJ., editors. Vol. 1134. Springer; New York: 2014. p. 103-130.chap. 9
37. Vander Heiden MG, Cantley LC, Thompson CB. Understanding the Warburg effect: the metabolic requirements of cell proliferation. Science. 2009; 324:1029–1033. [PubMed: 19460998]
38. Warner LM, Adams LM, Sehgal SN. Rapamycin prolongs survival and arrests pathophysiologic changes in murine systemic lupus erythematosus. Arthritis Rheumv. 1994; 37:289–297.
39. Suwannaroj S, Lagoo A, Keisler D, McMurray RW. Antioxidants suppress mortality in the female NZB x NZW F1 mouse model of systemic lupus erythematosus (SLE). Lupus. 2001; 10:258–265. [PubMed: 11341102]
40. Lai Z-W, Hanczko R, Bonilla E, Caza TN, Clair B, Bartos A, Miklossy G, Jimah J, Doherty E, Tily H, Francis L, Garcia R, Dawood M, Yu J, Ramos I, Coman I, Faraone SV, Phillips PE, Perl A. N-acetylcysteine reduces disease activity by blocking mTOR in T cells of lupus patients. Arthritis Rheum. 2012; 64:2937–2946. [PubMed: 22549432]
41. McDonald G, Deepak S, Miguel L, Hall CJ, Isenberg DA, Magee AI, Butters T, Jury EC. Normalizing glycosphingolipids restores function in CD4+ T cells from lupus patients. J. Clin. Invest. 2014; 124:712–724. [PubMed: 24463447]
42. Yamaguchi R, Perkins G. Finding a panacea among combination cancer therapies. Cancer Res. 2012; 72:18–23. [PubMed: 22052464]
43. Yao J, Chen S, Mao Z, Cadenas E, Brinton RD. 2-deoxy-D-glucose treatment induces ketogenesis, sustains mitochondrial function, and reduces pathology in female mouse model of Alzheimer's disease. PLoS ONE. 2011; 6:e21788. [PubMed: 21747957]
44. Nath N, Khan M, Paintlia MK, Singh I, Hoda MN, Giri S. Metformin attenuated the autoimmune disease of the central nervous system in animal models of multiple sclerosis. J. Immunol. 2009; 182:8005–8014. [PubMed: 19494326]
45. Telang S, Clem B, Klarer A, Clem A, Trent J, Bucala R, Chesney J. Small molecule inhibition of 6-phosphofructo-2-kinase suppresses T cell activation. J. Transl. Med. 2012; 10:95. [PubMed: 22591674]
46. Cheong J-H, Park ES, Liang J, Dennison JB, Tsavachidou D, Nguyen-Charles C, Wa Cheng K, Hall H, Zhang D, Lu Y, Ravoori M, Kundra V, Ajani J, Lee J-S, Ki Hong W, Mills GB. Dual inhibition of tumor energy pathway by 2-deoxyglucose and metformin is effective against a broad spectrum of preclinical cancer models. Mol. Cancer Ther. 2011; 10:2350–2362. [PubMed: 21992792]
47. Viollet B, Guigas B, Sanz Garcia N, Leclerc J, Foretz M, Andreelli F. Cellular and molecular mechanisms of metformin: an overview. Clin. Sci. 2012; 122:253–270. [PubMed: 22117616]
48. Dufort FJ, Bleiman BF, Gumina MR, Blair D, Wagner DJ, Roberts MF, Abu-Amer Y, Chiles TC. Cutting edge: IL-4-mediated protection of primary B lymphocytes from apoptosis via Stat6-dependent regulation of glycolytic metabolism. J. Immunol. 2007; 179:4953–4957. [PubMed: 17911579]
49. Del Prete A, Zaccagnino P, Di Paola M, Saltarella M, Oliveros Celis C, Nico B, Santoro G, Lorusso M. Role of mitochondria and reactive oxygen species in dendritic cell differentiation and functions. Free Radic. Biol. Med. 2008; 44:1443–1451. [PubMed: 18242195]
50. Everts B, Amiel E, Huang SC, Smith AM, Chang CH, Lam WY, Redmann V, Freitas TC, Blagih J, van der Windt GJ, Artyomov MN, Jones RG, Pearce EL, Pearce EJ. TLR-driven early glycolytic reprogramming via the kinases TBK1-IKK? supports the anabolic demands of dendritic cell activation. Nat. Immunol. 2014; 15:323–332. [PubMed: 24562310]
51. Xu Z, Cuda CM, Croker BP, Morel L. The NZM2410-derived lupus susceptibility locus Sle2c1 increases TH17 polarization and induces nephritis in Fas-deficient mice. Arthritis Rheum. 2011; 63:764–774. [PubMed: 21360506]

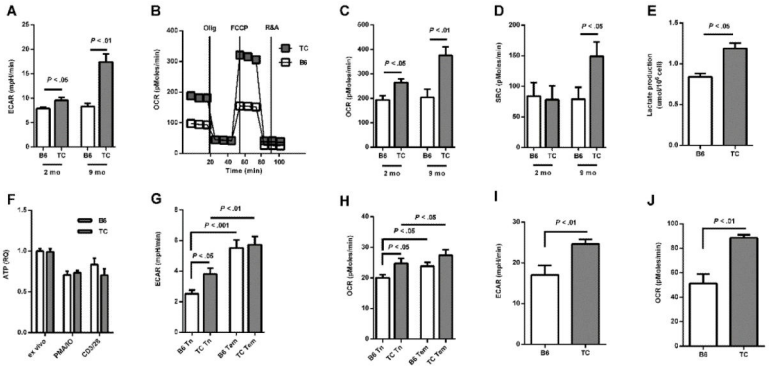

Figure 1.

$CD4^+$ T cells from TC mice show an enhanced metabolism. ECAR (**A**), OCR (**B, C**), and SRC (**D**) measured in total $CD4^+$ T cells from 2 and 9 month old B6 and TC mice. (**B**) Representative OCR in 9 month old B6 and TC $CD4^+$ T cells. (**E**) Extracellular lactate production from 3 month old B6 and TC $CD4^+$ T cells. (**F**) ATP production by B6 and TC $CD4^+$ T cells stimulated with PMA/ionomycin or anti-CD3/CD28. ECAR (**G**) and OCR (**H**) in Tn and Tem from 9 month old B6 and TC mice. ECAR (**I**) and OCR (**J**) in B6 and TC Tn after 24 h stimulation with anti-CD3/CD28. $N = 3$-6.

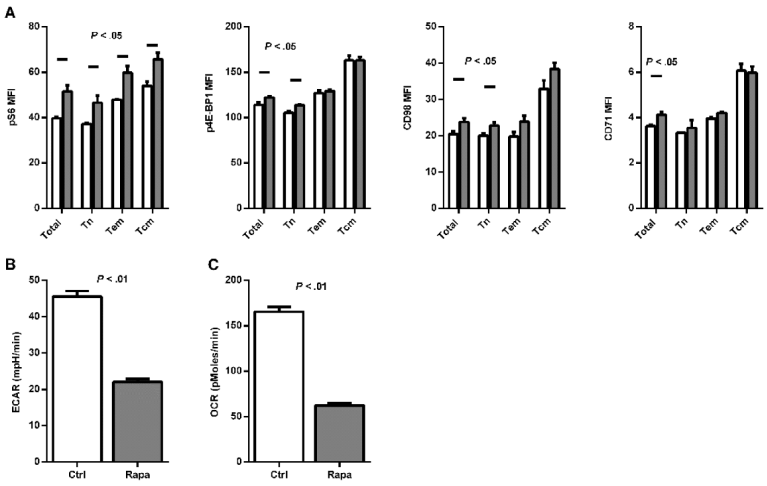

Figure 2.

$CD4^+$ T cells from TC mice show an increased mTORC1 activity. (**A**) S6 and 4E-BP1 phosphorylation and expression of CD98 and CD71 in total $CD4^+$ T cells as well as Tn, Tem and Tcm subsets from 2 month old mice. N = 3-4. (**B**) ECAR and OCR in B6 $CD4^+$ T cells stimulated with anti-CD3/CD28 with or without rapamycin (100 nM) for 24 h. Representative graphs of 2 independent assays each performed with N =7 technical replicates.

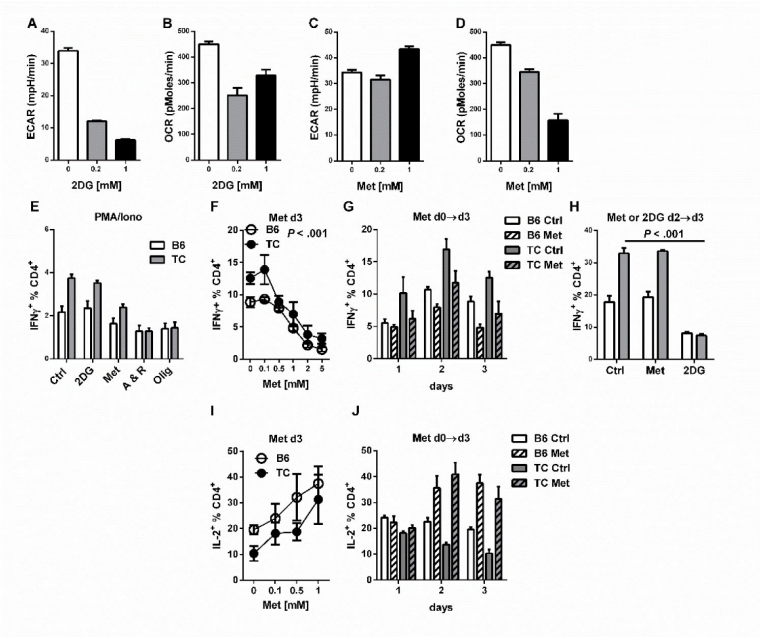

Figure 3.

Metabolic modulators normalized TC CD4$^+$ T cell effector functions *in vitro*. ECAR (**A**, **C**) and OCR (**B**, **D**) in B6 CD4$^+$ T cells stimulated with anti-CD3/CD8 for 24 h in the presence of 2DG or Met. Representative graphs of 3 assays each performed with technical replicates. (**E**) IFNγ production in CD4$^+$ T cells stimulated with PMA/Ionomycin/GolgiPlug for 6 h (Ctrl), in the presence of Met (2 mM), 2DG (5 mM), antimycin A/retonone (both 0.5 uM), or oligomycin (1 uM). IFNγ production in CD4$^+$ T cells cultured under Th1 condition for 3 d with Met (0-5 mM in **F** or 1 mM in **G**) or 2DG (1 mM) added from d0 (**F, G**) or d2 (**H**). IL-2 production in CD4$^+$ T cells stimulated with anti-CD3/CD28 for 3 d with 0 – 1 mM (**I**) or 1 mM (**J**). Panel G shown the statistical significance of a 2-way ANOVA between B6 and TC. *N*=3-8.

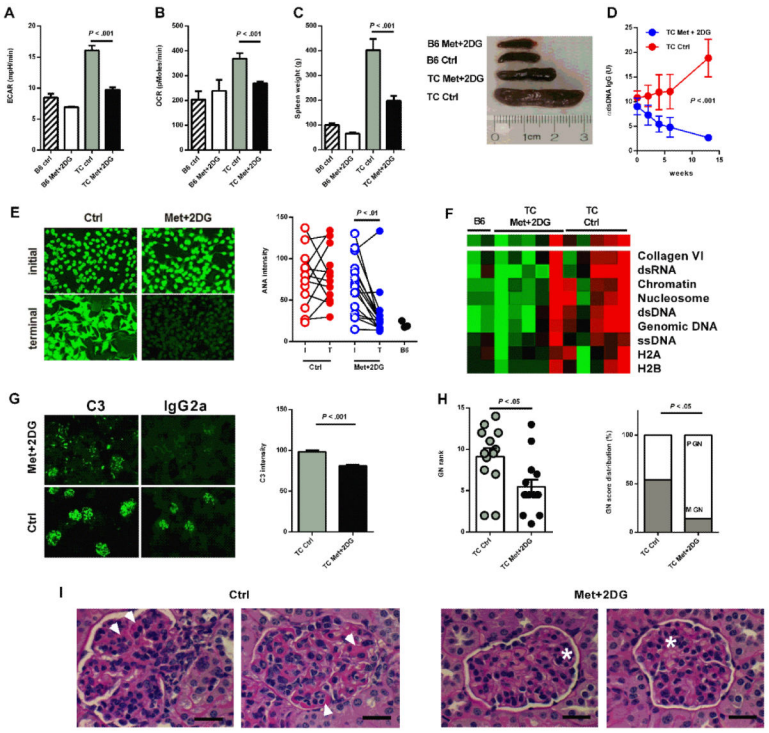

Figure 4.

Treatment with Met+2DG for 3 months reversed disease in 7 month old B6 and TC mice. (**A**) ECAR and (**B**) OCR in $CD4^+$ T cells. (**C**) Spleen weight (representative spleens on the right of 14 for TC and 5 for B6) (**D**). Serum anti-dsDNA IgG in TC mice (2-way ANOVA). (**E**) Initial (I) and terminal (T) serum ANA from TC mice. Representative images of 14 sera per group and ANA intensity quantification, with each linked symbol representing a mouse. Untreated B6 mice are shown as control (paired *t*-tests). (**F**) Autoantibody microarray analysis of terminal sera (IgG). (**G**) Immune complex deposition in TC glomeruli. Representative images of 14 kidneys per group with C3 and IgG2a deposits (left) and C3 intensity (3-6 glomeruli per mouse). (**H**) Renal pathology assessed by severity rank (median and interquantile range, 2-tailed Mann-Whitney test) and GN score distribution (χ^2 test). (**I**) Representative glomeruli (PAS stain) from untreated mice (left) showing large subendothelial deposits (arrows), and from treated mice (right) showing open capillaries and reduced hypercellularity (stars) (scale bars = 25 μm). *N=14* TC and 5 B6 mice per group.

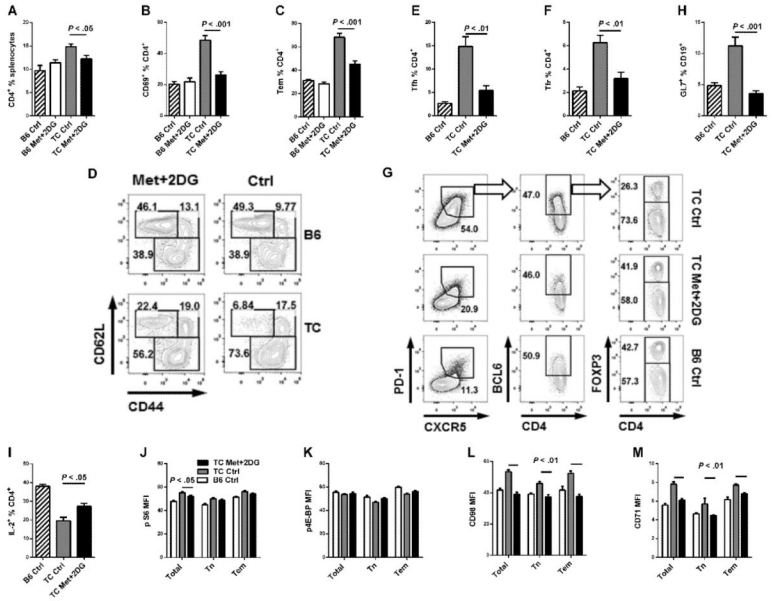

Figure 5.

A 3-month Met+2DG treatment normalized CD4$^+$ T cell phenotypes in aged TC mice. Percentage of total splenic CD4$^+$ T cells (**A**), CD69$^+$ (**B**) and Tem (C) CD4$^+$ T cells in B6 and TC treated and control mice. (**D**) Representative CD4$^+$-gated FACS plots showing the CD62L$^+$ CD44$^-$ Tn and CD62$^-$ CD44$^+$ Tem subsets. Frequency of Tfh (**E**) and Tfr (**F**) CD4$^+$ T cells, and representative CD4$^+$-gated FACS plots showing the PD-1^{hi} CXCR5^{hi} BCL6$^+$ Foxp3$^-$ Tfh and PD-1^{hi} CXCR5^{hi} BCL6$^+$ Foxp3$^+$ Tfr subsets (**G**). (**H**) Frequency of GC CD19$^+$ B cells. (**I**) IL-2 production in CD4$^+$ T cells stimulated with anti-CD3/CD28 for 24 h. (**J**-**M**) Effect of treatment on phosphorylation of S6 (**J**) and 4E-BP1 (**K**), as well as expression of CD98 (**L**) and CD71 (**M**) in total, Tn, and Tem T cells. N = 4-14.

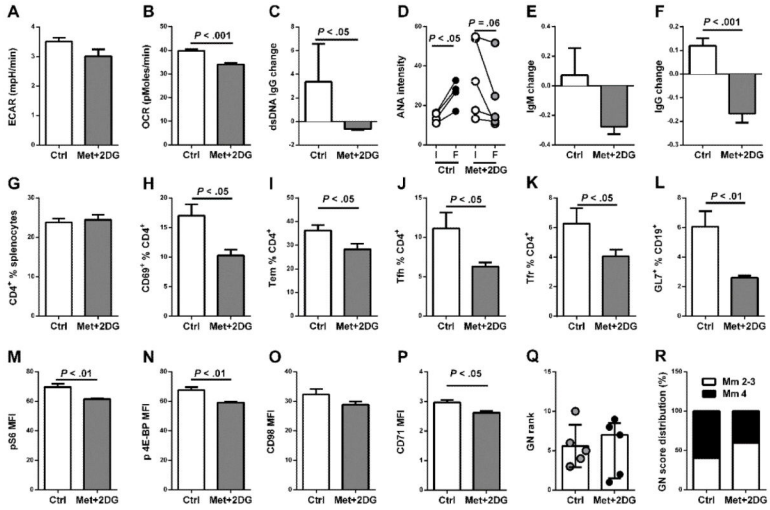

Figure 6.

Met+2DG treatment for one month reversed immunophenotypes in NZB/W mice. ECAR (**A**) and OCR (**B**) in splenic $CD4^+$ T cells. (**C**) Change between the terminal and the initial serum anti-dsDNA IgG for each mouse. (**D**) Serum ANA intensity with each linked symbol representing the initial and final value for each mouse. Change between the terminal and initial total serum IgM (**E**) and IgG (**F**). Frequency of total $CD4^+$ T cells (**G**), $CD69^+$ (**H**), Tem (**I**), Tfh (**J**) and Tfr (**K**) $CD4^+$ T cells and GC B cells (**L**). (**M**-**P**) Effect of treatment of mTORC1 targets: Phosphorylation of S6 (**M**) and 4E-BP1 (**N**) and expression of CD98 (**O**) and CD71 (**P**) in total $CD4^+$ T cells. Renal pathology assessed by severity rank (**Q**, median and interquantile range) and distribution of GN mesangial (Mn 2-3 and 4) scores (**R**). N = 4-5.

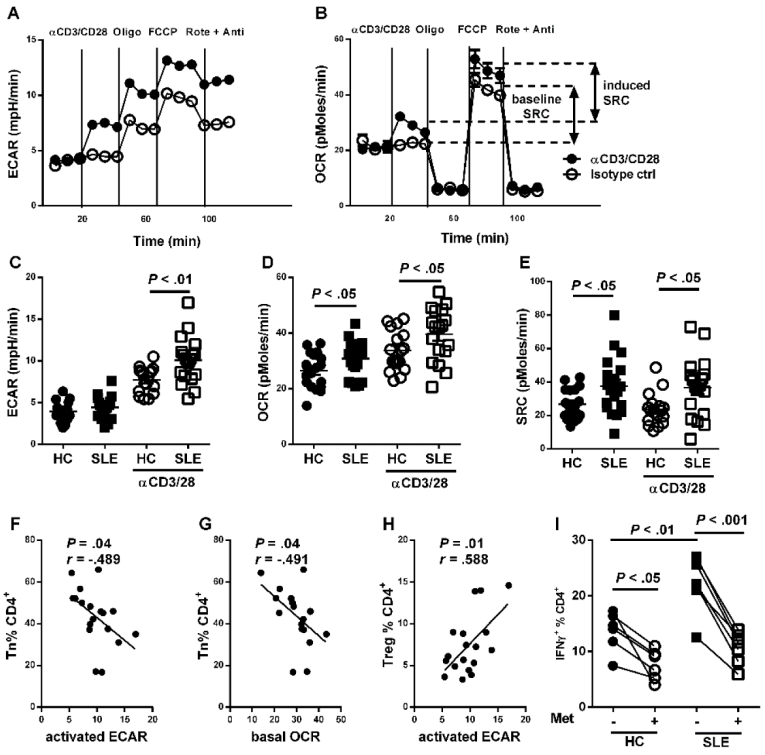

Figure 7.

CD4$^+$ T cells from SLE patients have an enhanced metabolism. Representative ECAR (**A**) and OCR (**B**) graphs of human CD4$^+$ T cells during a mitochondrial stress test. Anti-CD3/CD28 or isotope controls, oligomycin, FCCP and antimycin A/retonone were added to the cells as indicated. (**B**) ECAR (**C**), OCR (**D**) and SRC (**E**) in HC and SLE CD4$^+$ T cells, with and without anti-CD3/CD28 activation. *N*=19 HC and 20 SLE. Correlations between Tn percentages and activated ECAR (**F**) or basal OCR (**G**), and between Treg percentages and activated ECAR (**H**). For **F-H**, the significance and correlation coefficient of Pearson tests are shown. (**I**) IFNγ production in Th1-polairized CD4$^+$ T cells with or without Met. 2-tailed paired *t*-tests compared the effect of treatment within each cohort. *N* = 6.